doi:10.1016/j.jmb.2006.10.055 J. Mol. Biol. (2007) 366, 461–468

JMB

Available online at www.sciencedirect.com

ScienceDirect

ELSEVIER

Lipid Chain Selectivity by Outer Membrane Phospholipase A

Ann Marie Stanley[1], Anthony M. Treubrodt[1], Pitak Chuawong[2] Tamara L. Hendrickson[2] and Karen G. Fleming[1]*

[1]*T.C. Jenkins Department of Biophysics, Johns Hopkins University, 3400 North Charles Street, Baltimore MD 21218, USA*

[2]*Department of Chemistry Johns Hopkins University 3400 North Charles Street Baltimore, MD 21218, USA*

**Corresponding author*

Outer membrane phospholipase A (OMPLA) is a unique, integral membrane enzyme found in Gram-negative bacteria and is an important virulence factor for pathogens such as *Helicobacter pylori*. This broad-specificity lipase degrades a variety of lipid substrates, and it plays a direct role in adjusting the composition and permeability of bacterial membranes under conditions of stress. Interestingly, OMPLA shows little preference for the lipid headgroup and, instead, the length of the hydrophobic acyl chain is the strongest determinant for substrate selection by OMPLA, with the enzyme strongly preferring substrates with chains equal to or longer than 14 carbon atoms. The question remains as to how a hydrophobic protein like OMPLA can achieve this specificity, particularly when the shorter chains can be accommodated in the binding pocket. Using a series of sulfonyl fluoride inhibitors with various lengths of acyl chain, we show here that the thermodynamics of substrate-induced OMPLA dimerization are guided by the acyl chain length, demonstrating that OMPLA uses a unique biophysical mechanism to select its phospholipid substrate.

Keywords: membrane protein; thermodynamics; protein-protein interactions; OMPLA; protein-lipid interactions

Introduction

One of the challenges in understanding membrane proteins at a molecular level is to explain how, in a hydrophobic environment, these molecules achieve specificity and stability in their intra- and intermolecular interactions. These interactions depend, in part, on the relationship of the membrane proteins with their surrounding lipids; relevant lipid properties can range from bulk features of the bilayer, such as hydrophobic thickness,[1,2] to the requirement for specific lipids.[3–6]

As lipid is both its substrate and solvent, outer membrane phospholipase A (OMPLA) is a unique example in which specific lipid association modulates membrane protein interaction. Highly conserved among Gram-negative bacteria, OMPLA is activated in situations of stress, such as phage-induced lysis or heat shock;[7] when active, it can degrade a number of different lipids (Figure 1). Although enzymatically active only as a dimer,[8] OMPLA is largely monomeric in the absence of substrate.[8,9] However, covalent modification of the active-site serine with a substrate analog, hexadecylsulfonyl fluoride (HSF), induces OMPLA dimerization (Figure 2).[10] In the crystal structure of the covalently modified dimer (1QD6), two copies of HSF are seen bound in symmetry-related and chemically identical active-site clefts on opposite edges of the dimer interface (Figure 2(b)).[10] Presumably, the increased stability of the dimer is a result of the increase in intermolecular van der Waals interactions upon lipid binding and mimicked by the substrate analog.

In contrast to many soluble phospholipases, in which the lipid headgroup is an important specificity determinant,[11–13] OMPLA tolerates a wide-variety of substrate headgroups (Figure 1).[14] Instead, for

Abbreviations used: C14-SB, 3-(*N*,*N*-dimethylmyristylammonio)propanesulfonate; C12-SB, 3-(dodecyldimethylammonio)propanesulfonate; DEAE, diethylaminoethyl; DSF, decylsulfonyl fluoride; FF, fast flow; GpA, glycophorin A; HSF, hexadecylsulfonyl fluoride; LSF, laurylsulfonyl fluoride; NSF, nonylsulfonyl fluoride; OMPLA, outer membrane phospholipase A; OS, occluded surface; OSF, octylsulfonyl fluoride; pOSF, perfluorinated octyl sulfonyl fluoride; TM, transmembrane; USF, undecylsulfonyl fluoride.

E-mail address of the corresponding author: Karen.Fleming@jhu.edu

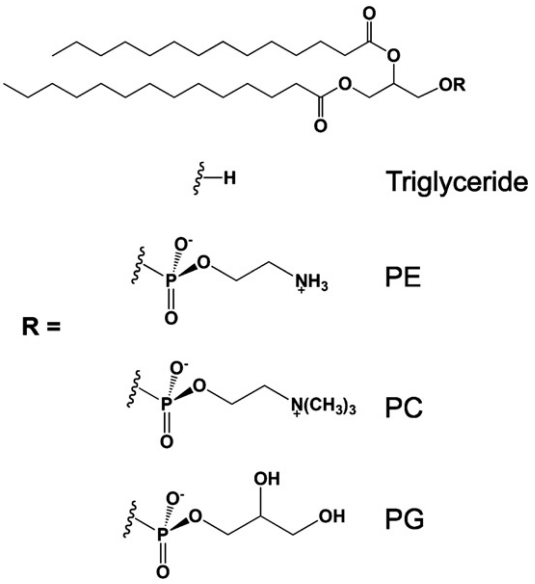

Figure 1. Chemical structures of OMPLA substrates. OMPLA shows little selectivity towards the lipid headgroup and is capable of hydrolyzing lipids with headgroups of different sizes and different charge properties. It is active on substrates including triglyceride, phosphatidylethanolamine (PE), phosphatidylcholine (PC), and phosphatidylglycerol (PG).[14]

OMPLA, the acyl chain length governs substrate selection, and it shows a marked preference for substrates with acyl chain lengths greater than or equal to 14 carbon atoms;[14] this selectivity suggested that perhaps it was only the terminal carbon atoms of long acyl chains that interacted with both subunits of the dimer. Paradoxically, occluded surface calculations on the crystal structure of OMPLA modified with HSF reveal that intermolecular contacts between the substrate analog acyl chain and the opposing subunit are distributed almost evenly along the length of a 16 carbon chain.[15] Therefore, the question remains as to how OMPLA can discriminate between substrates only by their acyl chain length. To explore the lipid chain selectivity and its role in OMPLA dimerization and activation, we synthesized a series of acyl sulfonyl fluoride inhibitors (Figure 2(a)) and determined their effects on OMPLA dimerization. We show here that there is a steep dependence of dimer stability on the substrate analog acyl chain length that explains the lipid chain selectivity.

Results

The dimer stability displays an unusual sigmoidal dependence on the substrate analog acyl chain length

Using sedimentation equilibrium analytical ultracentrifugation, we measured the free energy of dimerization of OMPLA as a function of the acyl chain length of the sulfonyl inhibitors. The use of covalent substrate analog inhibitors provides an important advantage in examining the energetic effects of acyl chain length on dimerization. Since OMPLA is a transmembrane protein, the lipid substrate acts also as solvent; therefore, changing the composition or concentration of the lipid in a titration experiment would change the solvent. By using covalent inhibitors, we were able to perform all experiments in an identical solvent environment of 2.5 mM C14-SB detergent micelles.

OMPLA was reacted separately with each of the inhibitors (Figure 2(a)), and we first determined the free energies of dimerization in the presence of 20 mM $CaCl_2$, a co-factor required for activity.[14] Calcium modestly stabilizes the overall enzyme dimerization,[8,15] which allowed us to explore a greater range of chain lengths. The free energy of association in each sedimentation equilibrium experiment was determined by global non-linear least-squares analysis of nine data sets, which is detailed in Materials and Methods. As described for HSF-modified OMPLA,[9] the sedimentation equilibrium data for OMPLA modified with our series of acyl sulfonyl fluorides (octylsulfonyl fluoride (OSF), nonylsulfonyl fluoride (NSF), decylsulfonyl fluoride (DSF), undecylsulfonyl fluoride (USF), laurylsulfonyl fluoride (LSF)) could be described well by a simple reversible monomer–dimer model. In analyzing the free energies of dimerization as a function of chain length, we discovered that the response of dimer stability as a function of chain length has a sigmoidal shape (Figure 3), which suggests that our measurements are not simply reporting on a uniform increase in packing interactions per unit chain length.

Results obtained in the presence of 20 mM EDTA suggest that this unusual dependence on chain length is not the result of cooperativity between calcium and the substrate analog (Figure 3). Because the OMPLA dimer is less stable in the absence of calcium,[9] we were able to measure monomer–dimer equilibria only for OMPLA modified with sulfonyl fluorides longer than C_{10} (DSF–HSF). For $n \leq 9$, the protein was entirely monomeric in the presence of EDTA under our experimental conditions. However, we previously estimated a lower limit to the stability in the absence of effector molecules, represented by the gray point in Figure 3.[9] While the curve in the presence of EDTA is not as well-defined as in the presence of calcium, the data still suggest a sigmoidal response of dimer stability to acyl chain length.

The linear region of the stability data has a surprisingly steep slope

For the results obtained in the presence of both calcium and EDTA, there is a range of the data for which the stability profile is approximately linear. For intermediate chain lengths of C_8–C_{12}, in the presence of 20 mM $CaCl_2$, the dependence of the free energy of dimerization on chain length can be

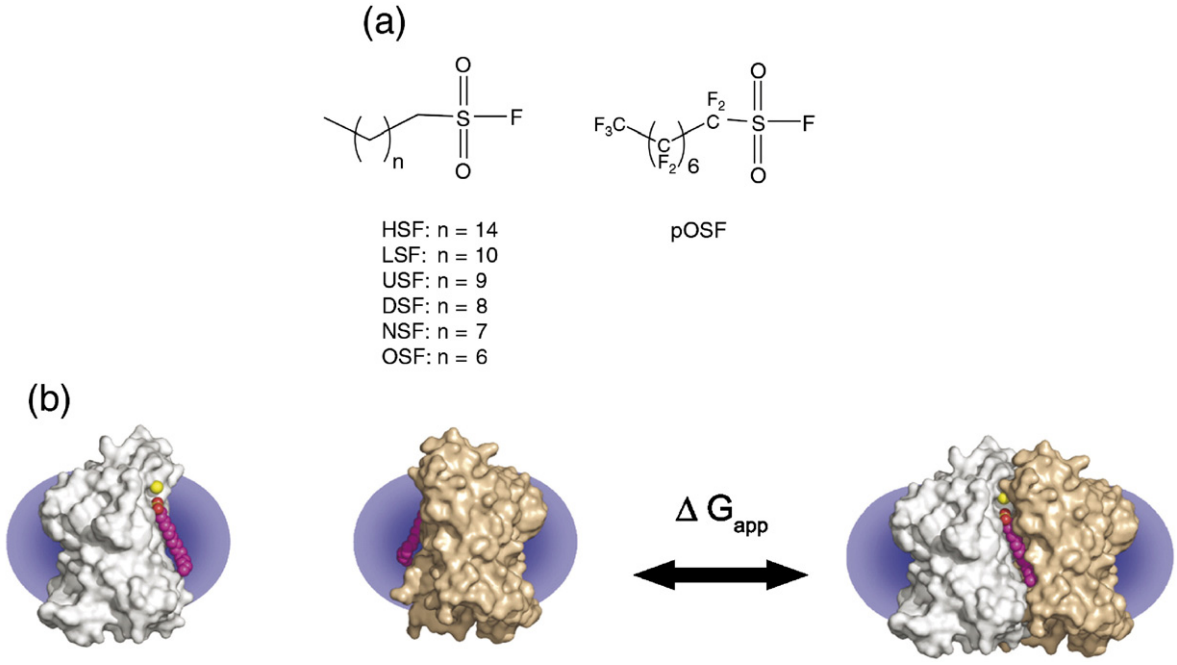

Figure 2. Substrate analog inhibitors of OMPLA. (a) The structures of the sulfonyl fluoride substrate analog inhibitors synthesized and used in this study are shown. A series of sulfonyl fluorides (SF) were synthesized, including: hexadecyl-(HSF), lauryl-(LSF), undecyl-(USF), decyl-(DSF), nonyl-(NSF), and octylsulfonyl fluoride (OSF). Perfluorinated octylsulfonyl fluoride (pOSF) was purchased from Sigma. (b) A schematic of the OMPLA dimerization equilibrium that is observed in the sedimentation equilibrium experiments, illustrating the change in environment of the acyl chain from the solvating micelle to the protein-binding pocket. The protein (1QD6) is shown in surface representation, the acyl chain of the hexadecylsulfonyl inhibitor is shown in CPK representation, and the blue circles represent the solvating micelles. This figure was generated using Pymol [http://www.pymol.org].

approximated by a straight line, which has a slope of -0.55 kcal mol^{-1} per methylene group (Figure 3, continuous line). For the intermediate values for which dimerization equilibria can be measured in the presence of 20 mM EDTA ($10 \leq n \leq 12$), the data can be fit with a line with a slope of -0.79 kcal mol^{-1} per methylene group (Figure 3, continuous line).

One framework for thinking about the enhancement in the free energy of OMPLA dimerization as a function of acyl chain length is to consider it in terms of transfer free energies of the acyl chain. Transfer free energies are often used to parameterize the hydrophobic effect and to relate the size of a hydrophobe to its energetics. In classic work, Tanford demonstrated that the transfer free energy of linear hydrocarbons from water to a hydrocarbon solvent depends linearly on the chain length with a slope equal to -0.88 kcal mol^{-1} per methylene group.[16] The energetics of pyruvate oxidase activation by monomeric amphiphiles also displays a linear dependence on acyl chain length that agrees well with Tanford's transfer free energies (-0.65 kcal mol^{-1} per additional methylene group);[17] this energy is believed to represent the transfer of the hydrophobic portion of the amphiphile from water to a hydrophobic binding site on the protein.

In contrast to the typical transfer free energies discussed above, the acyl chain in OMPLA would be transferred between two hydrophobic environments, e.g. from the solvating micelle to the protein interior (Figure 2(b)). It is therefore surprising that the energy differences for transfer of the substrate from the lipid micelle to the hydrophobic substrate binding pocket in OMPLA (a hydrophobic to hydrophobic transfer, -0.55 kcal mol^{-1} to -0.79 kcal mol^{-1} per methylene group) are so similar to those obtained by Tanford and in pyruvate oxidase studies (an aqueous to hydrophobic transfer, -0.65 kcal mol^{-1} to -0.88 kcal mol^{-1} per methylene group).[16–18] One explanation may be that the closeness of the values reflects hydration within the micelle.

The above values for transfer free energies per methylene group are derived assuming that the substrate analog acyl chain occupies the same position in the monomer as it does in the dimer, and that all intramolecular contacts between the acyl chain and its covalently attached subunit are formed in the monomer. In other words, upon dimerization only one-half of each methylene group goes from solvent-exposed to buried upon dimerization, while the back half of each methylene group remains occluded by its cognate subunit at all times. Alternatively, if the acyl chain does not make significant contact with its covalently attached subunit in the monomeric state, and both sides of the methylene group are exposed to the lipidic solvent, each incremental increase in inhibitor length may actually represent the net burial of two methylene groups. Therefore, it may be appropriate to divide the slopes we observe by 2 to give

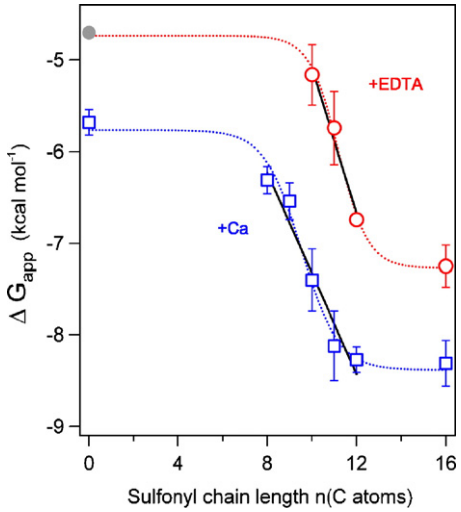

Figure 3. Response of dimer stability to acyl chain length. The free energy of OMPLA dimerization shows a sigmoidal dependence on the chain length of the covalently attached sulfonyl moiety that is consistent with the preference of OMPLA for long-chain substrates in both 20 mM calcium (blue squares) and 20 mM EDTA (red circles). Curve-fitting in IGOR Pro using the sigmoid option demonstrates this function is consistent with the data and is shown simply to emphasize the shape of the data (broken lines). The data can be approximated by a linear fit (continuous lines) for intermediate chain lengths ($8 \le n \le 12$ for calcium and $10 \le n \le 12$ for EDTA) to give slopes of $-0.55(\pm 0.07)$ kcal mol^{-1} per methylene ($R^2 = 0.95$) and $-0.79(\pm 0.12)$ kcal mol^{-1} per methylene ($R^2 = 0.95$) respectively.

-0.28 kcal mol^{-1} per methylene group ($CaCl_2$) to -0.40 kcal mol^{-1} per methylene group (EDTA). This analysis gives a lower limit to the transfer free energy per methylene group in our experiments; it reduces the slopes from the values observed in the Tanford transfer experiments significantly, supporting the hypothesis that the transfer of a lipid acyl chain from the micelle to the protein-binding pocket is less favorable than its transfer from water to a hydrophobic solvent. However, without additional information about the conformation of the substrate analog in the monomeric state, we are unable to distinguish between these two limits.

Notably, even the lower limits to our observed slopes are distinctly steeper than the chain length-dependence of interactions between lipids and membrane protein surfaces.[18] When measured in bilayers, the differential interactions between the surface of rhodopsin and lipids of different chain lengths showed a linear dependence with a slope of only -0.08 kcal mol^{-1} per methylene group. Similarly, association of lipid with the Ca-ATPase has been shown to have a dependence on chain length of only -0.04 kcal mol^{-1} per methylene group.[18] These observations suggest that the lipid interactions with the protein surface are similar to the interactions between the lipid chains themselves.[18] In contrast, the response of OMPLA dimer stability is at least five- to tenfold more sensitive to chain length than in these other systems. While there may be a contribution arising from the differences in the hydrophobic environments (bilayers *versus* detergent micelles), it is more likely that our results derive from the fact that the lipid-binding sites on OMPLA are true well-packed binding pockets for its substrate.

The steep increase in dimer stability at intermediate chain lengths does explain the high degree of discrimination that OMPLA can demonstrate towards short-chain substrates. For example, under the conditions of the centrifugation experiments, adding carbon atoms 9–12 to the substrate analog shifts the population of OMPLA from 35% dimer to over 80% dimer. Our data do suggest OMPLA would be as active on C_{12} substrates as on C_{14} or C_{16} substrates, but earlier biochemical work suggests OMPLA is not as active on C_{12} substrates as it is on their longer counterparts.[14] This could be due to a difference in the detergent environments used in the two sets of experiments. On the other hand, it could be that the chain length has other effects, for example on binding, that are captured in the activity assays but not in our covalent modification system. Nevertheless, the strong dependence of the stability of the active dimeric conformation on the acyl chain length is likely to be key in substrate selectivity.

The value for protein-acyl chain packing is more modest than that found for protein–protein interactions

How do the energetics of this specific lipid–protein interaction compare with those of membrane protein–protein interactions? To address this question, we normalized the slopes of the linear regions by the surface occluded on the acyl chain upon protein dimerization. While distinct from buried surface area, occluded surface area is a related parameter and can be interpreted as representing the molecular surface involved in intermolecular van der Waals contacts.[19] The free energy changes in the stability of helix–helix interactions for both bacteriorhodopsin and glycophorin A correlate strongly with the changes in buried surface area and/or occluded surface area.[20–22] It is believed that these correlations represent the value of van der Waals packing interactions.

Depending on whether the sulfonyl acyl chain makes contacts with monomeric OMPLA, 13–17Å^2 are occluded per methylene group in the dimer. In EDTA, this corresponds to an energy of -30 cal mol^{-1} Å^{-2} to -23 cal mol^{-1} Å^{-2}; in calcium, the values are -21 cal mol^{-1} Å^{-2} to -16 cal mol^{-1} Å^{-2}. The energy per Å^2 derived from transmembrane helix dimerization free energies for a series of glycophorin A sequence variants (38 cal mol^{-1} Å^{-2})[20,22] is as much as twofold higher than the values we calculate for the OMPLA protein–lipid interaction. We postulate this may reflect the higher entropic cost of immobilizing a freely rotatable acyl chain at an interface as compared to burying protein side-chains whose

rotational degrees of freedom are limited by the protein structure, but we believe that the energetics of the linear region are being dominated by van der Waals interactions.

The regions of turnover in the stability profile could arise from several factors

Although it is not clear what gives rise to the overall sigmoidal shape of our data, there could be several reasons to explain the regions of turnover. First, we are interpreting our results in terms of the structure of the HSF-modified OMPLA dimer (1QD6), but the structure in the presence of the shorter sulfonyl fluorides may differ. For example, it is possible that in the absence of an acyl chain, side-chains might move to fill in regions of the binding pocket. If these side-chains moved into positions occupied by carbon atoms 1–8 and 12–16 of the acyl chain in the sulfonylated dimer, then interactions at these carbon atoms in the modified dimer would not represent an increase in interactions over the unmodified dimer; this could explain the shallow slopes observed in these regions of the free energy graph. This idea is supported by molecular dynamics simulations of the OMPLA dimer in the absence of substrate, which showed amino acid side-chains moving into the substrate cleft and an overall collapse of the binding pocket.[23] However, the crystal structure of the monomer (1QD5) suggests that a rearrangement of the binding pocket may not be the explanation for the energetics we observe. The binding pocket appears pre-formed in the monomer, and the residues lining the pocket, particularly those that move in the simulation, adopt positions in the monomer nearly identical with their positions in the HSF-modified dimer.

Another explanation for the small difference in dimerization free energy between the unmodified and OSF-modified protein may be that that short carbon chains do not spend a significant time occupying the binding pocket. Even though the sulfonyl group is covalently attached, the active-site serine is on the edge of the protein dimer interface (Figure 2(b)), which may allow the acyl chain to swing out into the surrounding detergent. If the acyl chain is not occupying the binding pocket, then one would not actually gain additional intermolecular contacts upon sulfonylation with these shorter chains. It is possible also that for short acyl chains, a fraction of the dimer population has only one acyl chain bound and the acyl chain of the second HSF molecule adopts a conformation in which it extends into solvent and does not occupy the binding pocket. As the chain gets longer, the substrate analog would be bound more favorably and spend more time occupying the binding pocket, and, therefore, the packing interactions would contribute more significantly to the stability of the dimer.

The nearly constant free energy value between 12 and 16 carbon atoms could be explained also by the kink in the acyl chain observed in the crystal structure at carbon 12. The *gauche* conformation of this bond is unfavorable,[16,24] so any additional energy gained in packing interactions that is achieved between carbon atoms 12 and 16 may pay the cost for this kink yielding no net increase in stability of the OMPLA dimer. Overall, our results highlight the potential complexity in protein–lipid interactions; simply because methylene groups appear well-packed at the interface of a crystal structure does not mean they are undoubtedly a source of stability for the complex.

Perfluorination of the substrate analog acyl chain promotes aggregation

With our ability to modify OMPLA covalently with unnatural lipid analogs, we explored its response to a novel inhibitor, perfluorinated octyl sulfonyl fluoride (pOSF, Figure 2(a)). Probing the energetics of membrane protein interactions with fluorinated moieties is of particular interest because fluorinated compounds are both hydrophobic and lipophobic, and have potential utility in engineering membrane protein interactions.[25–27] Both SDS-PAGE analysis and sedimentation equilibrium analytical ultracentrifugation suggest that pOSF promotes a stronger association of OMPLA than its hydrogenated equivalent. The SDS-PAGE analysis reveals the presence of dimer in the pOSF-modified protein that is not apparent in the ordinary OSF-modified protein (Figure 4), and the apparent molecular mass returned by a single ideal species fit to centrifugation data was significantly larger than monomer in the presence and in the absence of calcium (Table 1).

However, in sharp contrast to the non-perfluorinated compounds, labeling with pOSF results in a loss of specificity and promotes aggregation. A ladder of bands corresponding to higher-order

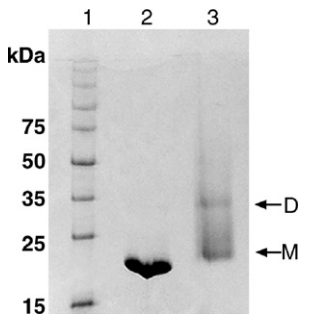

Figure 4. SDS-PAGE analysis of pOSF-modified OMPLA reveals the presence of dimers and higher-order species not seen in OSF-modifed OMPLA. Since SDS is a detergent micelle environment, membrane proteins may retain their structure, and stable non-covalent oligomers often remain associated. For each sample, 6 μg of protein eluted from a DEAE anion-exchange column in 7.5 mM C14-SB, 20 mM Tris (pH 8.3), 600 mM KCl was loaded onto a 12.5% polyacrylamide Phastgel, and the protein was visualized by staining with Coomassie bruilliant blue. Lane 1, markers; lane 2, OMPLA + OSF; lane 3 OMPLA + pOSF.

Table 1. Apparent molecular mass from single ideal species fits of sedimentation equilibrium analytical ultracentrifugation data for pOSF-Modified OMPLA

	+20 mM EDTA			+20 mM $CaCl_2$		
	Experiment number	Apparent molecular mass (kDa)	SRV	Experiment number	Apparent molecular mass (kDa)	SRV
+pOSF	1	49,631	8.33e-3	1	56,059	9.56e-3
	2	45,772	5.56e-3	2	51,069	7.20e-3
	3	52,926	1.00e-2	3	57,929	1.04e-2
+OSF	1	31,401	4.29e-3	1	42,109	5.33e-3
	2	28,891	5.72e-3	2	41,838	8.35e-3
	3	30,099	6.16e-3	3	39,887	6.06e-3

Monomeric OMPLA has a molecular mass of 31 kDa, and these results show, as with the SDS-PAGE analysis, that pOSF-modified OMPLA associates more than its hydrogenated counterpart. However, the high values for the SRV indicate that the data are poorly described by these single ideal fits.

oligomers was present in the SDS-PAGE pOSF lane, and were even more prominent in other samples (Supplementary Data Figure S1). Unlike the sedimentation equilibrium data for OMPLA modified with hydrogenated sulfonyl fluorides, which could be well-described by a simple monomer–dimer equilibrium model, the sedimentation equilibrium data for the pOSF data could not be fit to a unique model; the fits to the pOSF data were poor for a number of models, with large values for the square-root of the variance and non-random residuals (Supplementary Data Table S1). Only non-global monomer-separate dimer fits, which included an individual equilibrium constant for each data set, were able to describe the pOSF data well, indicating that the interactions of the pOSF-modified OMPLA were not reversible under the conditions of the centrifuge experiments.

Earlier studies found that partially fluorinated surfactants had more favorable interactions with the membrane protein than completely perfluorinated surfactants, which were unable to prevent aggregation.[28] Our results *via* covalent modification with pOSF suggest that an extensively fluorinated surface can promote undesirable aggregation. Thus, with regards to designing membrane–protein interfaces, it may be best to incorporate only moderate levels of fluorination at specific sites to promote partitioning from the hydrophobic solvent without promoting non-specific aggregation.

Conclusions

In conclusion, this combination of chemical and biophysical methods allowed us to dissect the impact of the acyl chain on OMPLA dimerization. The steep increase in the sigmoidal dependence of dimer stability on chain length explains the exquisite discrimination OMPLA can demonstrate towards chemically similar substrates and may represent a novel mechanism for molecular recognition of lipids by membrane proteins. Furthermore, our results highlight the potential complexity in protein–lipid interactions; simply because methylene groups appear to be well packed at the interface of a crystal structure does not mean they are undoubtedly a source of intermolecular stability.

Materials and Methods

Synthesis of sulfonyl fluorides

1-Hexadecanesulfonyl chloride (CAS 38775-38-1) was purchased from Aldrich. 1-dodecanesulfonyl chloride (CAS 10147-40-7), 1-octanesulfonyl chloride (CAS 7795-95-1), sodium 1-nonanesulfonate (CAS 35192-74-6), and sodium 1-undecanesulfonate (CAS 5838-34-6) were purchased from Lancaster synthesis. Sodium 1-decanesulfonate (13419-61-9), triphenylphosphine, and *N*-chlorosuccinimde were purchased from Sigma. For compounds for which the sulfonyl chloride precursor was available (HSF, LSF, OSF), the fluoride was prepared by reflux in acetone with ammonium fluoride as described.[29] For sulfonic acid precursors (NSF, DSF, USF), the sulfonyl fluoride was prepared by a two-step synthesis as described.[30] The chloride was generated by reaction of sulfonic acid with *N*-chlorosuccinimide and triphenylphosphine at room temperature. The acyl sulfonyl chloride was then refluxed in acetone with ammonium fluoride. Products were isolated over a silica column in 10% ether: hexanes, and the chemical identity was confirmed by proton NMR. Perfluoro-1-octanesulfonyl fluoride (CAS 307-35-7) was purchased from Aldrich.

Sulfonyl modification of OMPLA

OMPLA was purified from inclusion bodies as described.[29] Purified refolded OMPLA (1.5–2 mg) was exchanged by ion-exchange chromatography using DEAE Sepharose FF into 3 ml of a buffer containing 20 mM Tris–HCl (pH 8.3), 400 mM KCl, 5 mM C12-SB for labeling with sulfonyl fluorides. The protein elution was diluted into a final reaction buffer of 20 mM Tris–HCl (pH 8.3), 200 mM KCl, 2.5 mM C12-SB, 20 mM $CaCl_2$. A 12–50-fold molar excess of each acyl sulfonyl fluoride was added from a 50 mg/ml stock in $CHCl_3$ and allowed to react with protein overnight at room temperature on a rotator.

Complete modification of the protein by the sulfonyl fluoride was detected by monitoring loss of enzymatic activity using the colorimetric substrate 2-hexadecanoylthio-1-ethylphosphorylcholine (HEPC) from Cayman

Chemicals, coupled with Ellman's reagent. On average, 1–5 μg of OMPLA was assayed in 500 μl of 250 mM Tris–HCl (pH 8.3), 20 mM $CaCl_2$, 2.5 mM C12, 1 mM HEPC, and 1 mM 5,5′-dithiobis(2-nitrobenzoic acid) (DTNB).

Sedimentation equilibrium analytical ultracentrifugation

Sedimentation equilibrium experiments were performed in a Beckman XL-A analytical ultracentrifuge at 298K as described.[9] Data were collected at 280 nm for three initial concentrations of protein (10.0 μM, 6.6 μM, and 3.3 μM) and three rotor speeds (16,300 rpm, 20,000 rpm, and 24,500 rpm); the samples were centrifuged until equilibrium was reached, as determined by WINMATCH.† The density of the buffer, the partial specific volume of the protein, and the buoyant molecular mass of the protein were calculated using the software SEDNTERP.[31] For each experiment, the nine absorbance *versus* radial distribution profiles were analyzed globally using NONLIN;[32] the global fitting of the nine data sets to a single equilibrium constant is evidence for a reversible association reaction.[33] The equilibrium constants from NONLIN were converted to molar units using the molar extinction coefficient for OMPLA of $\varepsilon = 90444\ \text{mol}^{-1}\ \text{cm}^{-1}$,[29] and the free energy was calculated according to:

$$\Delta G_{\text{app}} = -RT\ln K_{\text{app}}$$

where R is the universal gas constant, T is temperature (in Kelvin), and K_{app} is the equilibrium constant. K_{app} is the equilibrium constant in molar units at a particular concentration of detergent and temperature (2.5 mM C14-SB and 298 K here) that is obtained directly from the sedimentation equilibrium experiments.[34] The free energies reported in Figure 3 are the averages of three independent experiments for each sulfonylated protein and the error bars in Figure 3 represent the standard deviation of the three experiments.

Occluded surface area calculations

Changes in occluded surface area, as well as changes in the closely related parameter of buried surface area, have been a useful means for parameterizing the energetics of transmembrane helix–helix interactions.[20–22] To compare the energetics of the OMPLA-acyl chain interactions with those of transmembrane protein–protein interactions, the surface area occluded on the acyl chain per atom was calculated from the crystal structure of the dimer (PDB 1QD6) using the OS 7.2.2 algorithm,[19] and a maximum ray length of 2.8 Å.

Acknowledgements

This work was supported by a grant from the NSF (MCB0423807) and by a Career award from the Department of Defense (DAMD17-02-1-0427). A.M.S. is a Howard Hughes Medical Institute Predoctoral Fellow. T.L.H. is supported by the National Institutes of Health (GM071480) and P.C. is supported by a DPST Fellowship from the Royal Thai Government.

† www.bbri.org/rasmb

Supplementary Data

Supplementary data associated with this article can be found, in the online version, at doi:10.1016/j.jmb.2006.10.055

References

1. Sparr, E., Ash, W. L., Nazarov, P. V., Rijkers, D. T., Hemminga, M. A., Tieleman, D. P. & Killian, J. A. (2005). Self-association of transmembrane alpha-helices in model membranes: importance of helix orientation and role of hydrophobic mismatch. *J. Biol. Chem.* **280**, 39324–39331.
2. Perozo, E., Kloda, A., Cortes, D. M. & Martinac, B. (2002). Physical principles underlying the transduction of bilayer deformation forces during mechanosensitive channel gating. *Nature Struct. Biol.* **9**, 696–703.
3. Zhang, W., Campbell, H. A., King, S. C. & Dowhan, W. (2005). Phospholipids as determinants of membrane protein topology. Phosphatidylethanolamine is required for the proper topological organization of the gamma-aminobutyric acid permease (GabP) of *Escherichia coli*. *J. Biol. Chem.* **280**, 26032–26038.
4. Zhang, W., Bogdanov, M., Pi, J., Pittard, A. J. & Dowhan, W. (2003). Reversible topological organization within a polytopic membrane protein is governed by a change in membrane phospholipid composition. *J. Biol. Chem.* **278**, 50128–50135.
5. Wang, X., Bogdanov, M. & Dowhan, W. (2002). Topology of polytopic membrane protein subdomains is dictated by membrane phospholipid composition. *EMBO J.* **21**, 5673–5681.
6. Bogdanov, M., Heacock, P. N. & Dowhan, W. (2002). A polytopic membrane protein displays a reversible topology dependent on membrane lipid composition. *Embo J*, **21**, 2107–2116.
7. Dekker, N. (2000). Outer-membrane phospholipase A: known structure, unknown biological function. *Mol. Microbiol.* **35**, 711–717.
8. Dekker, N., Tommassen, J., Lustig, A., Rosenbusch, J. P. & Verheij, H. M. (1997). Dimerization regulates the enzymatic activity of Escherichia coli outer membrane phospholipase A. *J. Biol. Chem.* **272**, 3179–3184.
9. Stanley, A. M., Chuawong, P., Hendrickson, T. L. & Fleming, K. G. (2006). Energetics of outer membrane phospholipase A (OMPLA) dimerization. *J. Mol. Biol.* **358**, 120–131.
10. Snijder, H. J., Ubarretxena-Belandia, I., Blaauw, M., Kalk, K. H., Verheij, H. M., Egmond, M. R. *et al.* (1999). Structural evidence for dimerization-regulated activation of an integral membrane phospholipase. *Nature*, **401**, 717–721.
11. Martin, S. F., Follows, B. C., Hergenrother, P. J. & Trotter, B. K. (2000). The choline binding site of phospholipase C (*Bacillus cereus*): insights into substrate specificity. *Biochemistry*, **39**, 3410–3415.
12. Snitko, Y., Han, S. K., Lee, B. I. & Cho, W. (1999). Differential interfacial and substrate binding modes of mammalian pancreatic phospholipases A2: a comparison among human, bovine, and porcine enzymes. *Biochemistry*, **38**, 7803–7810.

13. Nalefski, E. A., McDonagh, T., Somers, W., Seehra, J., Falke, J. J. & Clark, J. D. (1998). Independent folding and ligand specificity of the C2 calcium-dependent lipid binding domain of cytosolic phospholipase A2. *J. Biol. Chem.* **273**, 1365–1372.
14. Horrevoets, A. J., Hackeng, T. M., Verheij, H. M., Dijkman, R. & de Haas, G. H. (1989). Kinetic characterization of Escherichia coli outer membrane phospholipase A using mixed detergent-lipid micelles. *Biochemistry*, **28**, 1139–1147.
15. Stanley, A. M., Chuawong, P., Hendrickson, T. L. & Fleming, K. G. (2006). Energetics of outer membrane phospholipase A (OMPLA) dimerization. *J. Mol. Biol.* **358**, 120–131.
16. Tanford, C. (1991). *The Hydrophobic Effect: Formation of Micelles and Biological Membranes*. Krieger Publishing Company, Malabar, FL.
17. Blake, R. & Hager, L. P. (1978). Activation of pyruvate oxidase by monomeric and micellar amphiphiles. *J. Biol. Chem.* **253**, 1963–1971.
18. Marsh, D. (1995). Specificity of lipid-protein interactions. *Biomembranes*, **1**, 137–186.
19. Pattabiraman, N., Ward, K. B. & Fleming, P. J. (1995). Occluded molecular surface: analysis of protein packing. *J. Mo. Recogn.* **8**, 334–344.
20. Faham, S., Yang, D., Bare, E., Yohannan, S., Whitelegge, J. P. & Bowie, J. U. (2004). Side-chain contributions to membrane protein structure and stability. *J. Mol. Biol.* **335**, 297–305.
21. Doura, A. K., Kobus, F. J., Dubrovsky, L., Hibbard, E. & Fleming, K. G. (2004). Sequence context modulates the stability of a GxxxG-mediated transmembrane helix-helix dimer. *J. Mol. Biol.* **341**, 991–998.
22. Doura, A. K. & Fleming, K. G. (2004). Complex interactions at the helix-helix interface stabilize the glycophorin a transmembrane dimer. *J. Mol. Biol.* **343**, 1487–1497.
23. Baaden, M., Meier, C. & Sansom, M. S. (2003). A molecular dynamics investigation of mono and dimeric states of the outer membrane enzyme OMPLA. *J. Mol. Biol.* **331**, 177–189.
24. Schindler, H. & Seelig, J. (1975). Deuterium order parameters in relation to thermodynamic properties of a phospholiped bilayer. A statistical mechanical interpretation. *Biochemistry*, **14**, 2283–2287.
25. Bilgicer, B. & Kumar, K. (2004). *De novo* design of defined helical bundles in membrane environments. *Proc. Natl Acad. Sci. USA*, **101**, 15324–15329.
26. Bilgicer, B., Xing, X. & Kumar, K. (2001). Programmed self-sorting of coiled coils with leucine and hexafluoroleucine cores. *J. Am. Chem. Soc.* **123**, 11815–11816.
27. Naarmann, N., Bilgicer, B., Meng, H., Kumar, K. & Steinem, C. (2006). Fluorinated interfaces drive self-association of transmembrane alpha helices in lipid bilayers. *Angew. Chem. Int. Ed. Engl.* **45**, 2588–2591.
28. Breyton, C., Chabaud, E., Chaudier, Y., Pucci, B. & Popot, J. L. (2004). Hemifluorinated surfactants: a non-dissociating environment for handling membrane proteins in aqueous solutions? *FEBS Letters*, **564**, 312–318.
29. Horrevoets, A. J., Verheij, H. M. & de Haas, G. H. (1991). Inactivation of *Escherichia coli* outer-membrane phospholipase A by the affinity label hexadecanesulfonyl fluoride. Evidence for an active-site serine. *Eur. J. Biochem.* **198**, 247–253.
30. Kokotos, G., Kotsovolou, S., Constantinou-Kokotou, V., Wu, G. & Olivecrona, G. (2000). Inhibition of lipoprotein lipase by alkanesulfonyl fluorides. *Bioorg. Med. Chem. Letters*, **10**, 2803–2806.
31. Laue, T. M., Shah, B., Ridgeway, T. M. & Pelletier, S. L. (1992). Computer-aided interpretation of analytical sedimentation data for proteins. In *Analytical Ultracentrifugation in Biochemistry and Polymer* (Harding, S. E., Rowe, A. J. & Horton, J. C., eds), pp. 90–125, Royal Society of Chemistry, Cambridge.
32. Johnson, M. L., Correia, J. J., Yphantis, D. A. & Halvorson, H. R. (1981). Analysis of data from the analytical ultracentrifuge by nonlinear least-squares techniques. *Biophys. J.* **36**, 575–588.
33. Fleming, K. G. (2000). Probing stability of helical transmembrane proteins. *Methods Enzymol.* **323**, 63–77.
34. DeLano, W. L. (2002). The Pymol Molecular Graphics System, pp. http://www.pymol.org. DeLano Scientific, San Carlos, CA, USA.

Edited by J. Bowie

(Received 17 August 2006; received in revised form 11 October 2006; accepted 11 October 2006)
Available online 21 October 2006